DOI: 10.1021/ic901235n

Inorganic Chemistry
Article

Synthesis of Anatase TiO_2 Nanoshuttles by Self-Sacrificing of Titanate Nanowires

Hongkang Wang,[†] Wei Shao,[†] Feng Gu,[†] Ling Zhang,*[,†] Mengkai Lu,[‡] and Chunzhong Li*[,†]

[†]*Key Laboratory for Ultrafine Materials of Ministry of Education, School of Materials Science and Engineering, East China University of Science and Technology, Shanghai 200237, China, and* [‡]*State Key Laboratory of Crystal Materials, Shandong University, Jinan 250100, China*

Received June 26, 2009

Anatase TiO_2 nanoshuttles have been successfully prepared via a hydrothermal method under alkaline conditions by employing titanate nanowires as the self-sacrificing precursors. The experimental results showed that a radical structural rearrangement took place from titanate wires to anatase TiO_2 shuttles during the hydrothermal reaction on the basis of a dissolution−recrystallization process. The surface of titanate nanowires plays a key role in the transformation process by providing both the structural units (e.g., TiO_6 octahedra) to realize anatase transformation and locations for the deposition and rearrangement of the dissolved structural units, while the formation of shuttle morphology is attributed to the minimization of surface energy with thermodynamically stable (101) facets of anatase TiO_2. The shape and phase transformation process were foundto be dependent on the hydrothermal reaction time. Raman and photoluminescence spectra confirmed the crystalline nature of the TiO_2 nanoshuttles.

Introduction

Titanium dioxide (TiO_2), as one of the most important industrial materials, plays an important role in many applications such as photocatalysis,[1] dye-sensitized solar cells,[2] gas sensors,[3] biological coatings,[4] and Li ion battery materials.[5] In particular, one-dimensional (1D) TiO_2 nanostructures including nanowires and nanotubes have been widely investigated because of their unique physical and chemical properties originating from the one-dimensional structural confinement on the nanoscale.[6] Among 1D nanostructures, shuttle-like nanostructures have attracted great interest in recent years[7,8] due to their special optical properties such as excellent ultraviolet absorption and photoluminescence with promising applications in optical materials.[9−11] Various strategies have been developed for the synthesis of shuttle-like TiO_2 nanostructures.[12−14] For example, Chen et al.[14] reported the synthesis of shuttle-like TiO_2 nanocrystals using the microwave hydrothermal technique. Chu et al.[12] and Ambtus et al.[13] prepared shuttle-like TiO_2 via the hydrolysis of $TiCl_4$ under the designated pH value. As is known, there are many polymorphs of TiO_2, among which anatase is suggested to show better optoelectronic properties, for example, photocatalytic activity.[15−17] However, almost all of the reported TiO_2 nanoshuttles presented in the rutile phase. In 2008, Yang et al.[18] fabricated shuttle-like anatase TiO_2 through a hydrothermal method by using titanium isopropoxide as a titanium source and trithyl amine as a surfactant. Now, the investigation of the design and synthesis of anatase TiO_2 nanoshuttles with promising properties on a large scale, especially via such methods that may be easily controllable and repeatable, is still a challenge.

In recent years, diverse TiO_2 nanostructures with different morphologies (e.g., rod, wire, and tube) have been developed

*To whom correspondence should be addressed. E-mail: czli@ecust.edu.cn (C.L.), zlingzi@ecust.edu.cn (L.Z.).

(1) Indris, S.; Amade, R.; Heitjans, P.; Finger, M.; Haeger, A.; Hesse, D.; Grunert, W.; Borger, A.; Becker, K. D. *J. Phys. Chem. B* **2005**, *109*, 23274–23278.
(2) Zukalova, M.; Zukal, A.; Kavan, L.; Nazeeruddin, M. K.; Liska, P; Gratzel, M. *Nano Lett*. **2005**, *5*, 1789–1792.
(3) Liu, S. Q.; Chen, A. C. *Langmuir* **2005**, *21*, 8409–8413.
(4) Oh, S. H.; Finones, R. R.; Daraio, C.; Chen, L. H.; Jin, S. H. *Biomaterials* **2005**, *26*, 4938–4943.
(5) Armstrong, A. R.; Armstrong, G.; Canales, J.; Bruce, P. G. *Angew. Chem., Int. Ed*. **2004**, *43*, 2286–2288.
(6) Xia, Y. N.; Yang, P. D.; Sun, Y. G.; Wu, Y. Y.; Mayers, B; Gates, B.; Yin, Y. D.; Kim, F.; Yan, Y. Q. *Adv. Mater*. **2003**, *15*, 353–389.
(7) Thongchant, S.; Hasegawa, Y.; Wada, Y.; Yanagida, S. *Chem. Lett*. **2001**, *12*, 1274–1275.
(8) He, Z. B.; Yu, S. H.; Zhu, J. P. *Chem. Mater*. **2005**, *17*, 2785–2788.
(9) Chen, X. Y.; Cui, H.; Liu, P.; Yang, G. W. *Appl. Phys. Lett*. **2007**, *90*, 183118.
(10) Wu, X. Y.; Du, J.; Li, H. B.; Zhang, M. F.; Xi, B. J.; Fan, H.; Zhu, Y. C.; Qian, Y. T. *J. Solid State Chem*. **2007**, *180*, 3288–3295.
(11) Guo, Z. Y.; Du, F. L.; Li, G. C.; Cui, Z. L. *Cryst. Growth Des*. **2008**, *8*, 2674–2677.
(12) Chu, R. H.; Yan, J. C.; Lian, S. Y.; Wang, Y. H.; Yan, F. C.; Chen, D. W. *Solid State Commun*. **2004**, *130*, 789–792.
(13) Ambrus, Z.; Mogyorosi, K.; Szalai, A.; Alapi, T.; Demeter, K.; Dombi, A.; Sipos, P. *Appl. Catal., A* **2008**, *340*, 153–161.
(14) Chen, Z. Q.; Li, W. K.; Zeng, W. J.; Li, M. S.; Xiang, J. H.; Zho, Z. H.; Huang, J. L. *Mater. Lett*. **2008**, *62*, 4343–4344.
(15) Linsebigler, A. L.; Lu, G.; Yates, J. T. *Chem. Rev*. **1995**, *95*, 735–758.
(16) Fujishima, A.; Hashimoto, K.; Watanabe, T. *TiO2 Photocatalysis Fundamentals and Applications*; BKC Inc: Tokyo, 1999.
(17) Anpo, M. *Pure Appl. Chem*. **2000**, *72*, 1265–1270.
(18) Yang, C.; Yang, Z. M.; Gu, H. W.; Chang, C. K.; et al. *Chem. Mater*. **2008**, *20*, 7514–7520.

Published on Web 09/18/2009

through wet chemical treatment of alkaline titanates, which are promising precursors for the synthesis of TiO_2 nanostructures because of their open and layered structure and common structure features with anatase.[19−22] The phase and shape transformation mechanisms between titanate and titania under different reaction conditions have been studied. Zhu et al.[19] reported a composite structure of titanate fibers covered with anatase nanoparticles and ascribed the anatase transition partially to an in situ topochemical reaction, in which titanate nanofibers dehydrate due to the reaction with acid, accompanied by an in situ rearrangement of the structural units. Mao and Wong[23] suggested that the transformation of titanate nanostructures into their anatase titania counterparts is size- and shape-dependent under neutral hydrothermal conditions. Feng et al.[21] prepared a shuttle-like morphology of anatase TiO_2 nanocrystals transformed from layered titanate nanosheets with the axis of the shuttles parallel to that of the titanate nanosheets, by using an exfoliation technique under alkaline conditions. They ascribed the phase and shape transition to the synergistic effect of an in situ topotactic transformation reaction and a dissolution−deposition reaction. However, though much progress has been achieved, it can be found that the effects of exfoliating agents and alkaline pH value were not clearly clarified previously. Yang and Zeng[24] systhesized oriented anatase TiO_2 nanocrystals through the direct deposition of a titanium source (TiF_4) on protonated pentatinate nanobelts, which serve as templating materials for in situ nuclear formation and crystal growth of anatase. In this paper, we investigated the transition mechanism under alkaline conditions without the assistance of exfoliating agents, and we prepared anatase TiO_2 nanoshuttles by employing titanate nanowires as the sacrificing precursors. The phase and shape transition can be readily controlled by adjusting the hydrothermal reaction time. A delicate fishbonelike composite structure of titanate nanowire/anatase nanoshuttles, as an intermediate product, formed during the hydrothermal reaction, in which titanate nanowires are found to be covered by anatase TiO_2 nanoshuttles with the [001] directions perpendicular to the axis of the wires. Such an integrated composite with a specific organization pattern and shape of each component was suggested to further determine its ultimate physicochemical properties,[19,24−27] which maybe find broader practical applications.

Experimental Section

All chemicals were of analytical grade and used as received. In our experiment, titanate nanowires were synthesized by the alkaline hydrothermal process between a concentrated NaOH solution and titanium dioxide, initially developed by Kasuga et al.[28] The H-titanate was obtained by exchanging alkaline ions with protons using a dilute acid solution.[29] In a typical procedure, 3.0 g of commercial TiO_2 powder (Degussa P25) was dispersed in a 10 M NaOH aqueous solution, followed by hydrothermal treatment at 180 °C for 72 h in a Teflon-lined autoclave. The resulting white precipitate was washed thoroughly with distilled water and dried in the air at 80 °C overnight. The sodium titanate nanowires were then obtained. The H-titanate nanowires were obtained by exchanging Na ions with a 0.1 mol/L HCl aqueous solution through magnetic stirring for 24 h and then washed thoroughly with water (until the pH of the filtrate reached a value of ∼7), and they were subsequently air-dried at 80 °C overnight. To prepare the anatase TiO_2 nanoshuttles, 0.1 g of the as-prepared H-titanate nanowires was first dispersed in the distilled water, with a 1 M NaOH solution to adjust the solution to a desired alkaline pH value of 12. The pH-adjusted solution was transferred to a 50 mL autoclave, which was kept at 180 °C for 3−24 h. The resulting product was eventually collected by centrifugation, washed with distilled water, and finally dried in the air at 80 °C overnight. The yield of the product can be easily scaled up to 1.0 g by properly adjusting the reaction conditions.

X-ray powder diffraction (XRD) data were recorded on a Japan Rigaku D/max2550 VB/PC X-ray diffractometer system with graphite monochromatized Cu Kα irradiation (λ = 0.15418 nm). The morphology and structure were characterized by scanning electron microscopy (SEM; JEOL JSM-6460 microscope) images, transmission electron microscopy (TEM; JEM-2100), and high-resolution transmission electron microscopy (HRTEM, JEM-2010). Raman spectra of the powders were collected on a LabRam Infinity Raman spectrometer, using 785 nm lasers. The UV−vis absorption spectrum was measured on a Varian Cary500 UV−vis−NIR spectrophotometer. The excitation and photoluminescence spectra of the sample were measured with a Jobin Fluorolog-3-p spectrophotometer with a Xe lamp at room temperature.

Results and Discussion

Typical XRD patterns of the as-synthesized samples are illustrated in Figure 1. Figure 1a shows the XRD pattern of the titanate precursor, which could be indexed to a layered H-titanate with a monoclinic lattice ($C2/m$), according to the previous literature.[19,30−32] After hydrothermal treatment, the crystal phase changed greatly; all of the diffraction peaks matched well with the anatase phase of TiO_2 (JCPDS no. 21−1272; Figure 1b). Sharp diffraction peaks imply that the as-synthesized TiO_2 samples are crystalline. The Raman spectrum of the TiO_2 sample is shown in the inset of Figure 1. The Raman scattering peaks at 141, 195, 394, 513, and 637 cm^{-1} correspond with typical features of anatase TiO_2 single crystals.[33,34] The well-resolved, higher intensities of the

(19) Zhu, H. Y.; Gao, X. P.; Lan, Y.; Song, D. Y.; Xi, Y. X.; Zhao, J. C. *J. Am. Chem. Soc.* **2004**, *126*, 8380–8381.
(20) Kolen'ko, Y. V.; Kovnir, K. A.; Gavrilov, A. I.; Garshev, A. V.; Frantti, J.; Lebedev, O. I.; Churagulov, B. R.; Van Tendeloo, G.; Yoshimura, M. *J. Phys. Chem. B* **2006**, *110*, 4030–4038.
(21) Wen, P. H.; Itoh, H.; Tang, W. P.; Feng, Q. *Langmuir* **2007**, *23*, 11782–11790.
(22) Tsai, C. C.; Teng, H. *Langmuir* **2008**, *24*, 3434–3438.
(23) Mao, Y. B.; Wong, S. S. *J. Am. Chem. Soc.* **2006**, *128*, 8217–8226.
(24) Yang, H. G.; Zeng, H. C. *J. Am. Chem. Soc.* **2004**, *127*, 270–278.
(25) Valden, M.; Lai, X.; Goodman, D. W. *Science* **1998**, *281*, 1647–1650.
(26) Bell, A. T. *Science* **2003**, *299*, 1688–1691.
(27) Zeng, H. C. Nanostructured Catalytic Materials: Design and Synthesis. In *The Dekker Encyclopedia of Nanoscience and Nanotechnology*; Marcel Dekker: New York, 2004; pp 2539−2550.
(28) Kasuga, T.; Hiramatsu, M.; Hoson, A.; Sekino, T.; Niihara, K. *Langmuir* **1998**, *14*, 3160–3163.
(29) Sasaki, T.; Watanabe, M.; Hashizume, H.; Yamada, H.; Nakazawa, H. *J. Am. Chem. Soc.* **1996**, *118*, 8329–8335.
(30) Sasaki, T.; Nakano, S.; Yamauchi, S.; Watanabe, M. *Chem. Mater.* **1997**, *9*, 602–608.
(31) Bao, N. Z.; Lu, X. H.; Ji, X. Y.; Feng, X.; Xie, J. W. *Fluid Phase Equilib.* **2002**, *193*, 229–243.
(32) Chen, Q.; Du, G. H.; Zhang, S.; Peng, L. M. *Acta Crystallogr., Sect. B* **2002**, *58*, 587–593.
(33) Ohsaka, T.; Izumi, F.; Fujiki, Y. *J. Raman Spectrosc.* **1978**, *7*, 321–324.
(34) Busca, G.; Ramis, G.; Amores, J. M.; Escribano, V. S.; Piaggio, P. *J. Chem. Soc., Faraday Trans.* **1994**, *90*, 3181–3190.

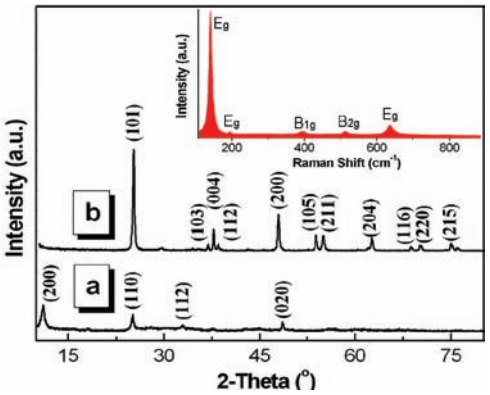

Figure 1. XRD patterns of titanate precursor (a) and anatase TiO_2 nanoshuttles (b) prepared using the hydrothermal method for 12 h. Inset shows the Raman spectrum of anatase TiO_2 nanoshuttles.

Raman peaks indicate that the as-prepared TiO_2 samples are highly purified with few defects.[35]

The SEM image of the titanate nanowires is shown in Figure 2a. The distinct wire morphology can be observed with lengths ranging from several hundreds of nanometers to several micrometers and a diameter of 30−200 nm. Figure 2b, c show the TEM images of TiO_2 nanoshuttles obtained after the hydrothermal treatment. It is clear that the wire morphology of the titanate precursor varied to a shuttle-like morphology with a diameter of ∼150 nm and a length of ∼250 nm. The electron diffraction (ED) pattern of the TiO_2 nanoshuttles in Figure 2d shows five diffusing rings, which can be indexed as diffraction from {101}, {004}, {200}, {211}, and {213} planes of anatase TiO_2, respectively. Figure 2e shows one randomly chosen TiO_2 nanoshuttle, and its corresponding HRTEM image is shown in Figure 2f. The lattice fringes of the shuttle are clearly observed, indicating that the nanoshuttle is single crystalline with good crystallinity. From the distance between the adjacent lattice fringes, an interplanar spacing of 0.35 and 0.48 nm matching well with (101) and (002) plane separations of anatase TiO_2 can be obtained. Also, the (002) plane is perpendicular to the axis direction of the TiO_2 nanoshuttles. Such features imply that the nanoshuttles grow along the (002) crystal plane with a preferred orientation in the [001] direction. The shuttle tip is confined by two sets of (101) planes, which is attributed to the lower surface energy of the (101) plane than that of other planes.[36] Therefore, it can be concluded that a radical structural rearrangement took place from titanate wires to anatase TiO_2 shuttles during the hydrothermal reaction. It is known that both titanate and anatase have common features in basic structural units (e.g., TiO_6 octahedra) and their combination modes. Two kinds of transformation mechanisms have been proposed for the transition from titanate to anatase: One is the in situ topochemical transformation mechanism,[19] in which layered titanate is transformed into anatase through the in situ dehydration reaction, where the pristine morphology of the titanate precursor is maintained after the reaction. The other is the dissolution/recrystallization mechanism,[21,37] where the hydrothermal treatment leads

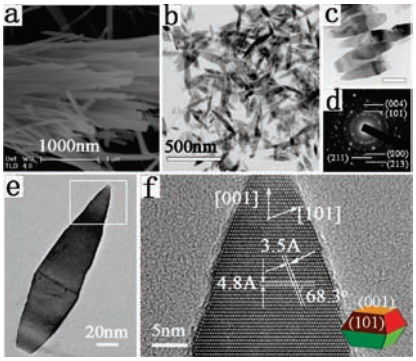

Figure 2. (a) SEM image of the titanate nanowires precursor. (b,c) TEM and ED results of the anatase TiO_2 nanoshuttles. (e,f) TEM and corresponding HRTEM image for a single shuttle. Inset of f denotes the relationship of (001) and (101) facets.

to the dissolution of the titanate precursor and formation of anatase TiO_2, which always results in a morphology change of the precursor. On the basis of the above observation, the present transformation evidently cannot attribute to an in situ topochemical reaction, which retains the pristine morphology of the precursor.[19,21]

The structure and morphology of the samples are found to be largely dependent on the hydrothermal reaction time. Figure 3a shows the TEM image of the sample obtained with hydrothermal treatment for 3 h under the same alkaline conditions (pH = 12). Interestingly, a delicate fishbonelike composite structure of titanate nanowires/anatase nanoshuttles formed with the precursor titanate nanowires perpendicularly covered by shuttlelike products with lengths of 100−200 nm. The XRD result shown in Figure 3c indicates that there exists both titanate and anatase in the products, forming an anatase/titanate composite. With increasing the reaction time further to 6 h, the titanate wire almost disappears along with the formation of ordered nanoshuttle arrays presented in the products. XRD patterns shown in Figure 3c also demonstrated that, once the hydrothermal time reached 6 h, the phase of the products varied from titanate to anatase TiO_2. Accordingly, with the hydrothermal reaction proceeding, the supporting titanate nanowires were consumed gradually with the formation of shuttle-like crystals, in which the titanate nanowires served as precursors and substrates and sacrificed themselves to form the nanoshuttles, confirming that the transformation is a dissolution−recrystallization process under hydrothermal conditions.[21] To better understand the phase and shape transitions, (HR)TEM measurements were taken to study the anatase/titanate composite structure and their surface contact state. Figure 4a shows the low-magnification TEM image of the anatase/titanate composite, and the nanoshuttle can be indexed to anatase TiO_2 with the [001] direction perpendicular to the axis of the nanowire (Figure 4b). The HRTEM results shown in Figure 4 reveal distinctly different lattices of the nanowire and nanoshuttle. Also, the nanowires can be indexed to the trititanate phase in the monoclinic $C2/m$ space group, using the $H_2Ti_3O_7$ unit cell parameters,[20,38] which can also be confirmed by Raman spectroscopy (Figure S1, Supporting Information). It is known that the trititanate phase has unit layers composed of three edge-shared TiO_6 octahedra, in which each unit of

(35) Zhao, Y. N.; Lee, U. H.; Suh, M.; Kwon, Y. U. *Bull. Korean Chem. Soc.* **2004**, *25*, 1341–1345.
(36) Song, M. Y.; Ahn, Y. R.; Jo, S. M.; Kim, D. Y.; Ahn, J. P. *Appl. Phys. Lett.* **2005**, *87*, 113113.
(37) Feng, Q.; Hirasawa, M.; Yanagisawa, K. *Chem. Mater.* **2001**, *13*, 290–296.
(38) Feist, P T; Davies, P. K. *J. Solid State Chem.* **1992**, *101*, 275–295.

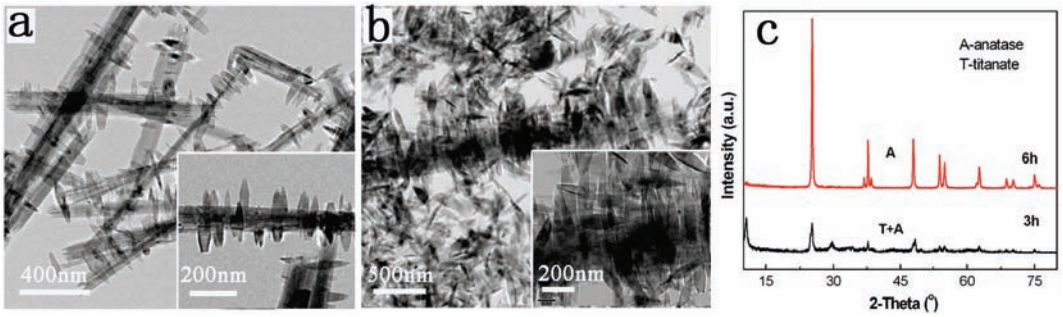

Figure 3. TEM images of the samples obtained with different hydrothermal reaction times: (a) 3 h, (b) 6 h. (c) Corresponding XRD patterns.

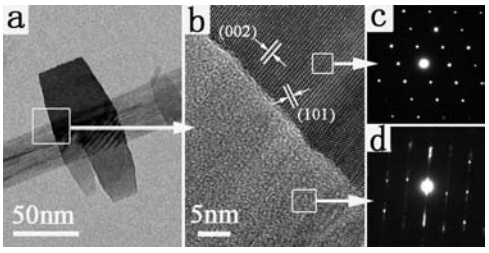

Figure 4. (a) TEM image of a typical composite structure of nanowire and nanoshuttle. (b) Corresponding HRTEM image of the boundary for the composite. (c,d) Corresponding ED patterns for the nanoshuttle and the nanowire.

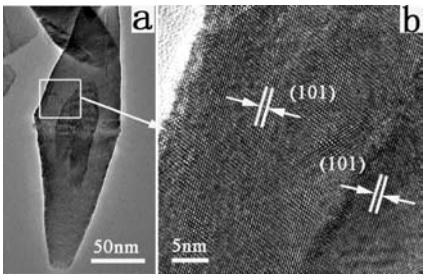

Figure 5. TEM image and corresponding HRTEM image of the sample after hydrothermal reaction for 24 h.

three TiO_6 octahedra is weakly linked through corner sharing.[39,40] This weakly chemical bonding nature of the precursor titanate may easily result in the rupture of the trititanate structure and dissolution into its unit layers, which is the precondition for the phase and shape transition. In addition, the existence of a high defect concentration in the titanate nanowires,[20] for example, stacking faults confirmed by SAED (Figure 4d), can benefit the rupture and sacrifice of the titanate wires precursor for a transformation to shuttle-like TiO_2 samples.

On the basis of the discussion, a possible transformation mechanism has been proposed for transformation from titanate nanowires to anatase TiO_2 nanoshuttles in the hydrothermal process. First, the titanate nanowires were dissolved into their elementary structural units such as TiO_6 octahedra or their layers under the role of concentrated hydroxyl groups[37](see Figure S2 for effects of pH on the products, Supporting Information). The dissolution began with the poor-crystalline locations from the outer to the inner layer gradually, and the deposition on the crystalline surface of the titanate nanowires happened simultaneously. The surface of the titanate nanowires may play a key role in the transformation process by providing the essential structural units to rearrange and realize anatase transformation through gradually dissolving, and by providing locations for the deposition and rearrangement of the dissolved structural units (Figure S3, Supporting Information). As both titanate and anatase have common features in the lattice structure containing zigzag ribbons of TiO_6 octahedra (sharing an edge with others to form an open octahedral framework[19,41]), the dissolved structural units can readily deposit on the TiO_6 octahedra layers on the specified crystal facets of the precursor titanate that mimic the anatase framework, through preffered nucleation enabled by appropriately controlling conditions.[24,42] Therefore, the existing TiO_6 octahedra layers of the precursor titanate serve as a seed layer for the epitaxial anatase crystals nucleating and growing along specific directions on the titanate surface.[24,42] From the HRTEM image (see Figure S4, Supporting Information), the coincident lattice fringes of the nanowire and nanoshuttle with parallel relation may indicate the first nucleation on the titanate surface, which induces the following oriented growth of anatase TiO_2. With the reaction proceeding, the titanate is finally dissolved and completely transformed to anatase under alkaline conditions. In addition, the TEM image shown in Figure 5a illustrates one TiO_2 nanoshuttle accompanied by a small unit attached to its surface, which is the intermediate structure being developed to form a well-defined nanoshuttle. From the corresponding HRTEM image shown in Figure 5b, the identical lattice fringes between the shuttle and small particle indicate that the small particle is being nibbled by the large shuttle, finally resulting in the crystal growth. This result suggests that a dissolution−deposition reaction is ongoing during the shape transformation,[21,37] with smaller particles disappearing and larger ones growing, just as with the Ostwald ripening process. This thermodynamically driven spontaneous process occurs because larger particles are more energetically favored than smaller particles.[43] From the point of view of thermodynamics, crystal growth usually begins with highly reactive

(39) Sun, X. M.; Li, Y. D. *Chem.—Eur. J.* **2003**, *9*, 2229–2238.
(40) Paek, M. J.; Ha, H. W.; Kim, T. W.; Moon, S. J.; Baeg, J. O.; Choy, J. H.; Hwang, S. J. *J. Phys. Chem. C* **2008**, *112*(41), 15966–15972.
(41) Xu, C. Y.; Zhang, Q.; Zhang, H.; Zhen, L.; Tang, J.; Qin, L. C. *J. Am. Chem. Soc.* **2005**, *127*, 11584–11585.
(42) Yang, X. F.; Karthik, C.; Li, X. Y.; Fu, J. X.; Fu, X. H.; Liang, C. L.; Ravishankar, N.; Wu, M. M.; Ramanath, G. *Chem. Mater.* **2009**, *21*, 3197–3201.
(43) Ratke, L.; Voorhees, P. W. *Growth and Coarsening: Ostwald Ripening in Material Processing*; Springer: New York, 2002.

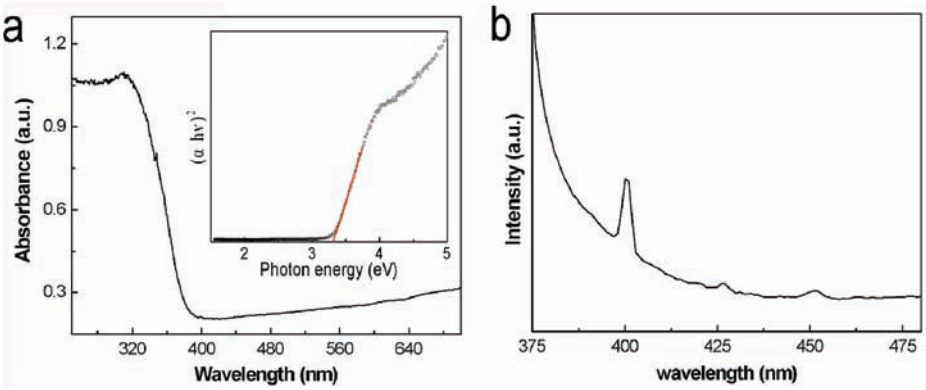

Figure 6. (a) UV−vis absorbance spectra of the TiO_2 nanoshuttles. The inset is a plot of $(\alpha h\nu)^2$ versus $h\nu$. (b) Photoluminescence spectrum of the anatase TiO_2 nanoshuttles. The excitation wavelength is 364 nm.

facets, which diminish rapidly as the crystal grows to minimize the surface energy.[44] For anatase TiO_2 crystals, (101) facets are thermodynamically stable with a surface energy of 0.44 J/m^2, much lower than that of (001) facets (0.90 J/m^2). Therefore, as TiO_2 nanocrystals grow without the existence of morphology-controlling agents, the active (001) facets disappear gradually and the stable (101) facets appear on the crystal surface until (001) facets completely disappeared at the end, resulting in the formation of the shuttlelike morphology with minimization of the surface energy (inset of Figure 2f).

The UV−visible absorption spectrum was carried out in order to characterize the optical absorbance of the anatase TiO_2 nanoshuttles. Figure 6a shows the absorption spectrum of the sample with a value of the absorption edge at 387 nm. The optical band gap energy can be estimated from the absorption spectra by using the following equation for a semiconductor:[45,46]

$$\alpha = \frac{k(h\nu - E_g)^{n/2}}{h\nu}$$

where α and E_g represent the absorption coefficient and the band gap, respectively. k is a constant, and n is equal to 1 for a direct transition. The band gap can be estimated from a plot of $(\alpha h\nu)^2$ versus photon energy ($h\nu$). The intercept of the tangent to the plot will give a good approximation of the band gap energy for this direct band gap material (shown in the inset of Figure 6a).[47] The band gap of the as-prepared TiO_2 nanoshuttles is calculated to be 3.31 eV, slightly larger than the value of 3.2 eV for the bulk TiO_2, which may be ascribed to the specially shuttlelike structural characteristics.[9]

Photoluminescence spectra were also recorded on the prepared TiO_2 nanoshuttles (Figure 6b). The emission spectrum possesses one sharp blue emission at 400 nm, which can be attributed to the radiative annihilation of excitons.[48] It is obvious that, besides the sharp blue emission, the curve is rather flat, and defect-related broad emission bands are hardly detected. As the dimensions of the anatase TiO_2 nanoshuttles are relatively larger, better crystallinity can be expected with fewer defects formed during the hydrothermal reaction, resulting in the disappearance of the defect-related emission.

Conclusions

Well-defined anatase TiO_2 nanoshuttles were prepared via a hydrothermal route by using titanate nanowires as self-sacrificing precursors. XRD, SEM, TEM, and HRTEM measurements were employed to investigate the phase and shape transformation process systematically. The experimental results showed that titanate wire was sacrificed to form anatase TiO_2 shuttles under a dissolution−recrystallization process. Due to the minimization of surface energy, the anatase TiO_2 nanoshuttle was formed by confinement with thermodynamically stable (101) facets. In addition, the delicate fishbonelike composite structure of titanate nanowire/anatase nanoshuttles may find practical applications in photocatalysts and separation.

Acknowledgment. This work was supported by the National Natural Science Foundation of China (2070-6015, 50703009), the Program of Shanghai Subject Chief Scientist (08XD1401500), the Major Basic Research Project of Shanghai (07DJ14001), the Shanghai Shuguang Scholars Tracking Program (08GG09), the Shanghai Rising-Star Program (09QH1400700), the Special Projects for Key Laboratories in Shanghai (09DZ2202000), the Special Projects for Nanotechnology of Shanghai (0852 nm02000, 0952 nm02100).

Supporting Information Available: Figures showing Raman spectra of the H-titanate nanowires precursor, typical TEM images of the products hydrothermally treated under neutral and acidic conditions, and SEM and (HR)TEM images of the composite structure. This material is available free of charge via the Internet at http://pubs.acs.org.

(44) Yang, H. G.; Sun, C. H.; Qiao, S. Z.; Zou, J.; Liu, G.; Smith, S. C.; Cheng, H. M.; Lu, G. Q. *Nature* **2008**, *453*, 638–642.
(45) Gu, F.; Wang, S. F.; Lu, M. K.; Zhou, G. J.; Xu, D.; Yuan, D. R. *J. Phys. Chem. B* **2004**, *108*, 8119–8123.
(46) Gu, F.; Wang, S. F.; Lu, M. K.; Zhou, G. J.; Xu, D.; Yuan, D. R. *Langmuir* **2004**, *20*, 3528–3531.
(47) Wang, Y.; Herron, N. *J. Phys. Chem.* **1991**, *95*, 525–532.
(48) Zhao, Y.; Li, C. Z.; Liu, X. H.; Gu, F.; Jiang, H. B.; Shao, W.; Zhang, L.; He, Y. *Mater. Lett.* **2007**, *61*, 79–83.